Determination of the Surface Tension and Surface Migration Constants for Tungsten*

J. P. Barbour, F. M. Charbonnier, W. W. Dolan, W. P. Dyke, E. E. Martin, and J. K. Trolan
Linfield Research Institute, McMinnville, Oregon

(Received October 1, 1959)

A determination of the surface tension and surface migration constants of metals in the solid phase, based on the use of pulsed field emission microscopy, is discussed. The experimental technique is described. An application to field emission cathodes of Herring's theory of transport phenomena in solids is given, which yields the necessary relations required for the determination of the basic physical constants from the experimental data. Results are presented and discussed for the case of tungsten. The method is applicable to a number of other metals, several of which are currently under investigation.

I. INTRODUCTION

TRANSPORT phenomena are known to occur in heated solids. Several physical processes may be involved, such as volume diffusion, evaporation and condensation, or plastic flow; the dominant process is determined by the experimental conditions, particularly the temperature and the size of the object under study. The experimental determination of the physical constants associated with transport phenomena provides basic information concerning the solid state; studies concerning refractory metals have a practical significance related to their use as cathode materials.

The evaporation of tungsten was studied some time ago by Zwikker.[1] More recently, tracer techniques have been used to investigate the volume self-diffusion of various metals, e.g., tantalum.[2] The surface migration of numerous combinations of impurities on base metals has been investigated with field emission microscopy.[3]

Recently, an intermediate temperature has been used to maintain the electrical stability and longevity of pulsed field emitters[4]; under such conditions, the tungsten emitter may change its shape by a transport mechanism which has been identified as surface migration.[5] The choice of operating conditions requires a knowledge of the diffusion constants and surface tension. Each of these constants may be determined with good accuracy through the measurement of the rate of change of cathode geometry. In an early experiment Müller[6] obtained an indirect determination of the geometric change from the corresponding change in the field emission current-voltage relationship, and deduced values for the activation energy and the diffusivity constant; uncertainties were introduced in these measurements by the lack of a sensitive method for the direct measurement of small geometrical changes, and by the inability to determine the emitter geometry accurately by direct observation.

Pulsed T-F emission microscopy[7] provides a considerably more sensitive method by which the rate of surface migration can be directly measured during the transport of a sufficiently small volume of material that the gross cathode geometry remains essentially unchanged. Other advantages of the method include a controlled and favorable cathode geometry, excellent depth resolution and high magnification, and continuous monitoring through the emission pattern of the surface under study. The present paper reports the use of this method to obtain improved values of the activation energy and diffusivity constant for tungsten, and also to determine the surface tension from the effect on the surface migration rate of an electrostatic surface stress; similar measurements are in progress for tantalum and molybdenum. The method is generally applicable to all materials from which field emission can be obtained, i.e., metals and semiconductors, and its use is particularly convenient in the case of refractory metals.

II. EXPERIMENTAL TECHNIQUE

The object selected here for the study of surface migration of tungsten-on-tungsten is the single crystal tip of a needle shaped field emission cathode ("emitter"). Such cathodes have an approximately spherical tip smoothly fitted to a conical shank; a typical emitter profile is shown in Fig. 1. Cathodes are sharpened by electropolishing and then smoothed and cleaned by controlled heating in vacuum[8]; the heating time and temperature can be adjusted to provide any desired value of the tip radius, within the approximate range 10^{-5} to 10^{-4} cm. The detailed shape of the cathode near the tip is obtained from electron microscope shadow-

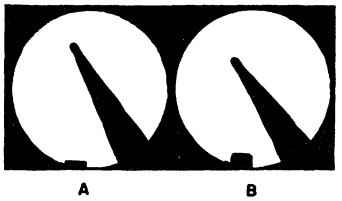

FIG. 1. Electron microscope shadowgraphs of a typical field emitter. *B* shows emitter rotated 90° from position of *A*.

* This work was supported by the U. S. Navy, Office of Naval Research, and was reported, in part, at the 1955 and 1956 Field Emission Symposia.

[1] C. Zwikker, Physica **5**, 249 (1925).
[2] D. B. Langmuir, Phys. Rev. **86**, 642(A) (1952).
[3] R. H. Good, Jr., and E. W. Müller, in *Handbuch der Physik*, edited by S. Flügge (Springer-Verlag, Berlin, 1956), Vol. XXI, pp. 176–231.
[4] W. P. Dyke et al. (to be published).
[5] J. L. Boling and W. W. Dolan, J. Appl. Phys. **29**, 556 (1958).
[6] E. W. Müller, Z. Physik **126**, 642 (1949).
[7] W. P. Dyke and J. P. Barbour, J. Appl. Phys. **27**, 356 (1956).
[8] W. P. Dyke et al., J. Appl. Phys. **24**, 570 (1953).

graphs,[8] and cathodes with symmetry of revolution are selected for the measurements. The surface curvature is maximum at the apex, and the very large curvature gradients near the emitter tip lead to high surface migration rates; since the cathode has symmetry of revolution the direction of the curvature gradient is known, and its magnitude may be measured on the cathode shadowgraph. When the cathode is heated transport phenomena are activated and in the absence of electric field material migrates from the emitter apex toward the shank; in the present work migration rates are determined from the corresponding changes in emitter length.

The field emission cathode is mounted in a projection microscope, with the emitter tip at the center of a spherical bulb coated with an aluminum-backed phosphor. Field emission occurs at the tip when sufficient voltage is applied to the phosphor screen, and the emitted electrons strike the screen, yielding an emission pattern characteristic of the crystallographic structure of the cathode material.[9] Observation of this pattern gives a ready determination of the crystal orientation at the emitter tip; it permits elimination of cathodes having crystal boundaries near the tip, and it provides an estimate of the degree of purity of the surface under study. Emission patterns have been extensively used for the study of metal surfaces, and particularly for the study of the adsorption, migration and desorption of foreign adsorbates on a pure metal substrate,[3] when such adsorbates affect the work-function and therefore cause visible changes in the emission pattern; however, simple observation of the pattern does not allow the quantitative study of self-diffusion processes.

The usefulness of the field emission projection microscope in the study of transport phenomena is greatly enhanced by the use of pulse techniques.[7] When the screen voltage is applied in short pulses, a suitable combination of pulse length and repetition rate (e.g., one-microsecond pulses applied at a rate of 30 pulses per second) provides visual continuity of the emission pattern while minimizing the disturbing effect on surface migration of the electric field at the emitter tip. It is then possible to draw large pulsed current densities and to obtain patterns in which the emission from lattice steps of atomic height (e.g., 2.23 A for the (110) crystal planes of a tungsten emitter surface) can be detected by a corresponding bright ring. As surface migration proceeds, atoms migrate from the apex toward the emitter shank, and a repetitive process occurs in which the uppermost atom layer is dissolved and the corresponding ring shrinks and disappears. It has been shown that each collapsing ring corresponds to the removal of a single atom layer from the emitter tip.[10] Thus the change in emitter length which occurs during a given period of time can be determined with high accuracy by counting the number of rings which collapse during the same period. The rate of change in emitter length and the corresponding surface migration rates are thus accurately determined by measuring the "ring rate" over the period required for the dissolution of about 50 atom layers at the emitter tip; since the emitter radius is large compared with this change, the observation is made at essentially constant geometry. This contributes considerably to the accuracy of the experiment in view of the sensitive dependence of migration rate on emitter radius, as will be developed in the next section. Also a series of successive measurements, e.g., to determine the variation with temperature of the migration rate and the corresponding activation energy, may be performed with the same emitter, thus allowing greater accuracy by eliminating the effect of small errors in the determination of emitter geometry. In this case the initial and final values of the emitter radius are obtained directly from electron microscope shadowgraphs of the emitter profile, and intermediate values corresponding to successive measurements are determined from the relationship between screen voltage and emitted current.

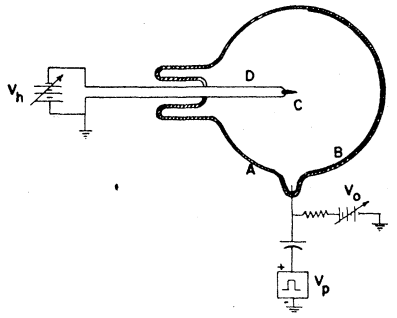

FIG. 2. Experimental field emission projection tube used in surface migration experiments (schematic illustration). A: glass envelope; B: aluminum back willemite phosphor anode; C: field emission cathode; D: cathode supporting filament. The emitter temperature is controlled through the variable voltage V_h; the steady-state bias field F_0 is controlled through the variable voltage V_0; a pulser supplies the low duty cycle voltage V_p required to produce a visible emission pattern on the anode screen.

Thus the use of pulsed field emission microscopy and the ring method allow a sensitive and accurate determination of the geometrical changes resulting from transport phenomena, which can be applied to a quantitative study of self-diffusion processes in single crystals of pure metals.

The experimental tube is shown in Fig. 2. A very high vacuum is desired in order to maintain a high degree of surface purity throughout the experiment. There are well-known methods for obtaining vacuums of the order of 10^{-12} mm Hg in sealed off tubes, and the methods used herein have been described in an earlier paper.[11] At such pressures the emitter surface is cleaned initially by a brief heat flash and remains clean for several hours during which data are obtained. Cathode temperatures were measured at the emitter shank (within 0.5 mm of the emitter tip) by a micro-optical pyrometer, and the

[9] E. W. Müller, Physik. Z. **37**, 838 (1936).
[10] J. K. Trolan et al., Phys. Rev. **100**, 1646 (1955).
[11] W. P. Dyke and J. K. Trolan. Phys. Rev. **89**, 799 (1953).

true tip temperature was then obtained from the calculated temperature drop along the shank. The calculated temperature correction is quite small. In order to check the accuracy of the calculation and the possible effect of thermomotive forces on the surface migration, one of the experimental tubes was built with an additional cylindrical electrode surrounding the emitter and maintained at the cathode filament temperature. Good agreement was found between the data obtained with both types of tubes.

While the electric field at the emitter tip was high during the pulse (e.g., 7×10^7 v/cm), the ratio of field-on time to total time (duty cycle) was 3×10^{-5}, i.e., sufficiently small that the pulsed electrostatic forces had no appreciable effect on the migration rate. This was confirmed by the observation that an increase in duty cycle to 3×10^{-4} produced no detectable change in the ring rate.

III. THEORY

Herring[12] has applied the principles of thermodynamics to the theoretical study of transport phenomena and of the associated geometric changes in heated crystals of pure metals. The resulting general expressions have then been applied to the conditions prevailing in field emission experiments, to provide the basis for the interpretation in terms of physical constants of the experimental measurements presented in the next section.

A. General Expressions

Starting from energy considerations, Herring has established the condition for the geometrical equilibrium of the solid-vacuum interface at the surface of an isothermal single crystal of arbitrary shape. The equilibrium condition is simply that the difference μ_M of the chemical potentials for atoms and lattice vacancies, evaluated at some point M just beneath the surface, be independent of the position of point M. Herring has derived the following expression for μ_M [13]:

$$\mu_M=\mu_0+\Omega_0\left[\gamma\left(\frac{1}{R_1}+\frac{1}{R_2}\right)+\frac{1}{R_1}\frac{\partial^2\gamma}{\partial n_1^2}+\frac{1}{R_2}\frac{\partial^2\gamma}{\partial n_2^2}-P_{xx}\right], \quad (1)$$

where Ω_0 is the volume per atom in cm^3, γ is the surface tension in dynes/cm, R_1 and R_2 are the principal radii of curvature of the metal surface just about the point M, n_1 and n_2 are the surface directions associated with the principal radii of curvature, and P_{xx} represents the normal component of any externally applied surface stress in dynes/cm^2; μ_M is expressed in ergs/atom, and μ_0 is an arbitrary constant which represents the value of μ below a stress-free plane surface.

Conversely, if μ_M is not a constant everywhere below the solid-vacuum interface the metal surface will alter its shape when heated, as a result of one or several atom transport processes such as volume diffusion or surface migration. Scaling laws, i.e., a comparison of the time durations required for the same relative geometrical change to take place in two geometrically similar aggregates, other parameters being equal, have been derived by Herring[14] for four possible processes. As was noted earlier, these laws have been used at this laboratory[5] to show experimentally that surface migration is the predominant transport process near the tip of tungsten field emission cathodes, under the conditions prevailing in the experiments described below; this results from the unusually small size and therefore high surface-to-volume ratio of the field cathode tip, and it permits a direct study of surface migration processes which in other experiments are often masked by volume diffusion.

In cases of small departures from equilibrium, the basic assumption is made that the rate of kinetic change of the surface is everywhere proportional to the gradient of the chemical potential, and Herring derives the basic expression for the flux of atoms $\mathbf{J}_M$ (in atoms/cm sec) at any point M on the surface:

$$\mathbf{J}_M=-\frac{D_0e^{-Q/RT}}{A_0kT}(\nabla\mu)_M, \quad (2)$$

where D_0 is the diffusivity constant in cm^2/sec for surface migration, Q is the activation energy in calories per mole, T is the crystal temperature in degrees Kelvin, A_0 is the surface area per atom and $(\nabla\mu)_M$ is the gradient at point M of the quantity μ_M given by Eq. (1).

B. Application to Field Emission Cathodes

The purpose of this section is to apply the general expressions to the case of field emitters, and more specifically to relate the time rate of change dz/dt of the emitter length to basic physical constants. As noted previously the geometry of the field cathode is such that surface migration predominates, other transport phenomena such as volume self-diffusion having only a negligible effect on the geometrical changes of the emitter for the range of temperatures investigated.

The previous equations show that the chemical potential μ_M, and therefore also the migration rates, may be changed by application at the cathode surface of an external stress which varies with position. The experimental arrangement used makes it possible to apply a known electrostatic stress, simply by application of a relatively small dc bias voltage at the phosphor screen; the larger field required for emission is then superimposed in the form of low duty cycle pulses.

Although in a strict sense some of the physical quantities appearing in Eqs. (1) and (2), such as A_0, D_0, Q or γ, are anisotropic because of the crystalline structure of the emitter material, the effects of this anisotropy

[12] C. Herring, in *Structure and Properties of Solid Surfaces*, edited by R. Gomer and C. S. Smith (University of Chicago Press, Chicago, 1953).

[13] C. Herring, in *The Physics of Powder Metallurgy*, edited by W. E. Kingston (McGraw-Hill Book Company, New York, 1951).

[14] C. Herring, J. Appl. Phys. **21**, 301 (1950).

for the metals considered here are relatively small except for a few specific orientations such as (110) and (211). Thus, in the present experiments where over-all migration rates are measured for surface migration paths involving large distances and a great number of surface orientations, the second order derivatives of the surface tension γ may be neglected to a good approximation in expression (1) for the chemical potential; assuming an external stress due only to electrostatic forces one obtains the simpler expression for the surface migration current $\mathbf{J}_M$ at some point M on the emitter surface:

$$\mathbf{J}_M=-\frac{\Omega_0^2}{A_0}\frac{D_0e^{-Q/RT}}{kT}\nabla_M\left[\gamma\left(\frac{1}{R_1}+\frac{1}{R_2}\right)-\frac{F^2}{8\pi}\right], \quad (3)$$

where $\mathbf{J}_M$ denotes the volume of material, in cm³/cm sec, which flows per unit time across a line of unit length perpendicular to the direction of the migration at point M, and ∇_M represents the gradient of the quantity in brackets, evaluated at point M. This gradient, and therefore also $\mathbf{J}_M$, are directed along meridian curves on the emitter surface since the emitter has symmetry of revolution. Equation (4) below is a convenient alternate form of Eq. (3), in which r is the radius of curvature of the emitter at the apex, F_0 is the applied electric field at the apex, a_M and c_M represent dimensionless coefficients which may depend only on the details of the emitter geometry and the particular point M considered.

$$J_M=-\frac{\gamma\Omega_0^2}{A_0}\frac{D_0e^{-Q/RT}}{kT}\frac{1}{r^2}a_M\left(1-\frac{1}{c_M}\frac{rF^2}{16\pi\gamma}\right). \quad (4)$$

1. *Migration in the Absence of Applied Electric Field: Thermal Etch*

In the absence of electric field forces the surface migration is controlled by the surface tension forces, and atoms migrate from the apex toward the shank of the emitter; this is readily understood since migration in that direction will reduce the surface energy. Figure 3 illustrates the position of the emitter surface at two successive instants; as surface migration proceeds the emitter length decreases and the emitter radius increases. It is observed experimentally that the rate of change of emitter length dz/dt is much larger than the corresponding rate of change of emitter radius dr/dt, a result expected in view of the emitter geometry. Thus in first approximation the rate of flow of material dv/dt across plane P perpendicular to the emitter axis, which by definition of J_M must be equal to $2\pi r_M J_M$, is also related to dz/dt by the expression:

$$(dV/dt)=\pi r_M^2(dz/dt), \quad (5)$$

and the following expression is obtained for the rate at which the emitter recedes in the absence of applied electric field:

$$\left(\frac{dz}{dt}\right)_0=\frac{2}{r_M}J_M=-\frac{\gamma\Omega_0^2}{A_0}\frac{D_0e^{-Q/RT}}{kT}\frac{1}{r^2}\frac{2a_M}{r_M}. \quad (6)$$

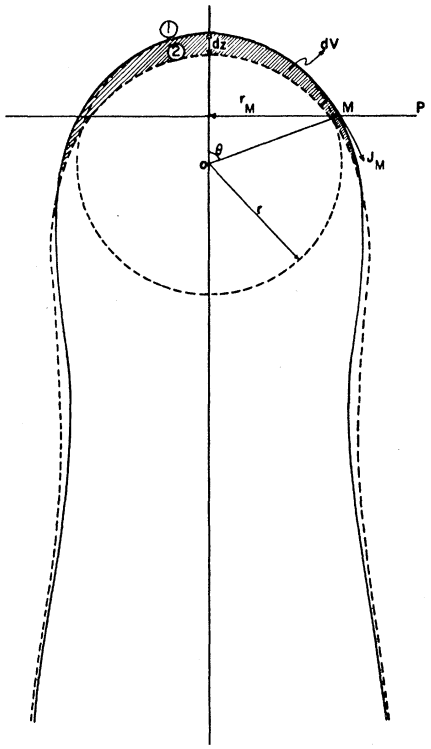

FIG. 3. Successive positions ① and ② of the field emitter surface.

Thus a value of the activation energy for the surface migration of tungsten on its own lattice can be obtained from the measured temperature dependence of the emitter receding rate; the determination of Q does not require precise knowledge of the emitter geometry.

In addition, graphical curvature measurements have been performed on the electron microscope shadowgraphs of several emitters. Within the accuracy of the measurements it is found that the quantity $2a_M/r_M$ is independent of the point M considered, at least up to $\theta=90°$, and shows only little variation from one emitter to another. Thus for the purpose of determining the diffusivity constant D_0 an average value $2a_M/r_M\cong 1.25/r$ may be substituted in Eq. (6), yielding the final expression:

$$\left(\frac{dz}{dt}\right)_0=-\frac{\gamma\Omega_0^2}{A_0}\frac{D_0e^{-Q/RT}}{kT}\frac{1.25}{r^3}. \quad (7)$$

2. *Migration in the Presence of Applied Field*

If a dc bias field is now applied at the emitter surface, the surface energy is reduced by an amount proportional to the square of the electric field. In view of the emitter geometry the field is maximum at the emitter apex and decreases toward the shank; therefore electrostatic forces will oppose the surface tension forces and will reduce the migration rate. This is in agreement with the basic Eq. (3), and a straightforward derivation leads to the expression for the emitter receding rate in the pres-

ence of a dc electric field having the value F_0 at the emitter apex:

$$\left(\frac{dz}{dt}\right)_{F_0}=\left(1-\frac{1}{c_0}\frac{rF_0^2}{16\pi\gamma}\right)\left(\frac{dz}{dt}\right)_0, \tag{8}$$

where c_0 is the value of the coefficient c_M at the apex. Thus the theory predicts that the emitter receding rate will decrease with dc applied field, by a relative amount proportional to the square of the field but independent of the field polarlty.[15] The field distribution at the emitter surface can be calculated by electrostatic theory[8] for a given emitter geometry, and an average value $c_0=0.5$ is then obtained by comparing the curvature and field gradients near the emitter apex. Thus the surface tension for the emitter material is obtained from the expression:

$$\gamma=rF_{01}^2/8\pi \tag{9}$$

in terms of the minimum field F_{01} required at the emitter apex to reduce the receding rate to zero. A practical significance is that when a steady-state field of this magnitude is applied the emitter may be heated to maintain electrical stability while avoiding emitter dulling.

If the dc applied field is further increased, electrostatic forces predominate over surface tension forces, the net surface migration currents are reversed and are now directed toward the emitter apex. According to Eq. (8) one might expect the emitter to extrude under such conditions; however, simple extrusion does not occur because of the difficulty of nucleating new atom layers in certain crystallographic directions, which prevents growth of the emitter in these directions. As a result, a more complicated process called "build-up" takes place, in which the initially rounded emitter gradually assumes a polyhedral shape. A discussion and experimental study of the build-up process is forthcoming in another paper[16]; in this case the simple theory given in this section, which treats the emitter material as being isotropic, does not apply.

[15] It may be noted that Eq. (8) is not strictly correct, because application of an electric field at the emitter surface causes a change not only in the chemical potential μ but also in the activation energy Q for surface migration. The latter effect arises because the activation energy is a measure of the difference between the potential energies of the migrating atom at a stable site and at the saddle separating two stable sites, and the migrating atom experiences a different electric field at the stable and saddle positions. This effect was first pointed out by J. A. Becker [Bell System Tech. J. **30**, 907 (1951)] and was studied in more detail by M. Drechsler [Z. Elektrochem. **61**, 48 (1957)]. This variation of Q with applied field does not change the field which reduces the emitter receding rate to zero, and it does not invalidate the Eq. (9) from which the surface tension is obtained; however it will cause a slight departure from linearity in the relationship between dz/dt and F^2. Calculations of the field effect on activation energy by a method similar to that of Drechsler show that the maximum variation from the zero field activation energy is less than 0.02 ev/atom or 0.6% for the fields of interest in the present work ($F_0 \leqslant 10^7$ v/cm), and may therefore be neglected without significant error in the derivation of Eq. (8); this is further confirmed by the experimental results shown in Fig. 5.

[16] P. C. Bettler and F. M. Charbonnier (to be published).

IV. EXPERIMENTAL RESULTS AND DISCUSSION

The receding rate of heated tungsten field emission cathodes has been measured as a function of temperature and dc applied field. The axis of the emitters used in these experiments coincides with a (110) crystallographic direction, and the emitter receding rate is determined from the rate at which bright emission rings collapse at the center of the emission pattern. As noted in Sec. II, the collapse of each ring corresponds to the dissolution by surface migration of one atom layer at the emitter apex; the corresponding reduction in length is $(\sqrt{2}/2)\times 3.16=2.23$ angstroms, since tungsten has a body-centered cubic structure with a lattice parameter of 3.16 A.

Figure 4 shows a typical plot of the time separation between the collapse of successive rings. At time t_0 the emitter temperature was reduced from T_1 to a smaller value T_2, with a corresponding increase in the time separation between rings. Apart from small statistical fluctuations due to the random nature of diffusion processes the ring rate (i.e., the reciprocal of the time interval separating the collapse of 2 successive rings) has a well-defined and reproducible steady-state value, for a given temperature T and dc bias field F_0 at the emitter tip; this steady state value (corresponding for instance to the segments AB or CD of the curve $ABCD$ shown in Fig. 4) is used, in conjunction with Eqs. (7) to (9), for the determination of the surface migration constants and the surface tension. In addition, a transient BC is observed following the time t_0 at which a change is made in either T or F_0. The transient has a duration Δt which

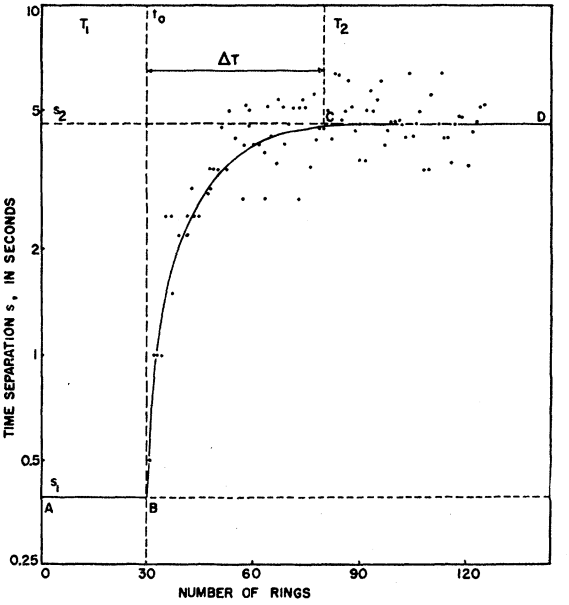

FIG. 4. Typical plot of the time separation s between the collapse of successive rings. At time t_0 the emitter tip temperature is reduced from $T_1=2750$°K to $T_2=2315$°K. Disregarding statistical fluctuations in the individual counts, the time separation s follows the curve $ABCD$.

is too long to be explained by the thermal inertia of the emitter tip; the transient corresponds to a number of rings which depends on the magnitude of the temperature or field change but is otherwise reproducible. These characteristics of the transient may be explained by noting that the detailed shape of the emitter surface depends on the relative values of the surface energy at different points; since the emitter material is slightly anisotropic, changes in temperature or surface field will modify the relative values of the surface energy and cause local rearrangements of the surface to adjust to a new equilibrium geometry. Such rearrangements are expected to be small in terms of the overall emitter geometry, and have therefore been ignored in the derivation of the expressions (7) and (8) for the steady-state migration rates (this view is supported by the good agreement between the functional relationships predicted by the theory and those measured experimentally, particularly with respect to the effect of a surface field on the steady state migration rate). On the other hand these temporary local rearrangements of the surface would be expected to affect the ring rate appreciably, because of their effect on the size of the small (110) plane facet at the emitter apex, and the transient observed in the ring rate is thought to arise from this effect.

The dependence of the receding rate on the magnitude of the dc applied field is shown in Fig. 5 for a typical emitter. The percentage of zero-field receding rate is plotted vs the square of the dc electric field at the emitter apex. The experimental points fall on a straight line, in agreement with Eq. (8) derived from the theory.

Using $r=5.5\times10^{-5}$ cm as obtained from electron microscope shadowgraphs of the emitter and the value $F_{01}=1.08\times10^{7}$ v/cm determined by the intercept of the experimental line with the x axis, one may calculate γ from Eq. (9). This procedure has been used with several emitters, and yields values of γ in the range 2700 to 3100

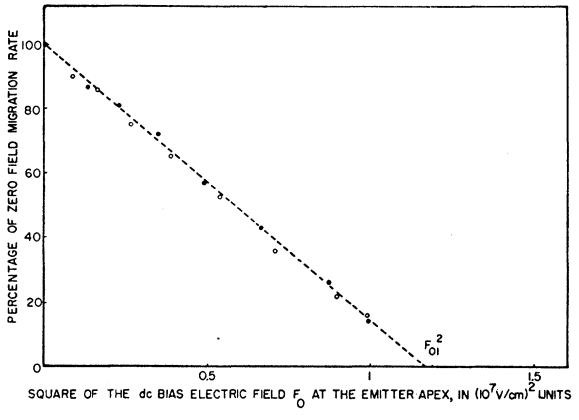

FIG. 5. Dependence of the emitter receding rate on the magnitude of the dc electric field applied at the emitter apex, for a fixed tip temperature (2030°K). ○—Run 1: bias field gradually increased from zero to a maximum value slightly larger than F_{01}. ●—Run 2: bias field gradually decreased from this maximum value down to zero.

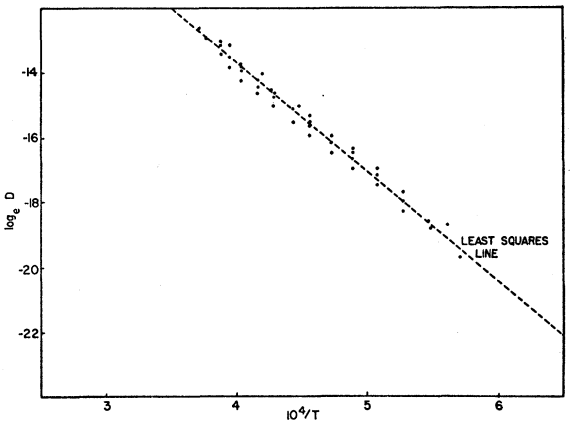

FIG. 6. Natural logarithm of the surface migration coefficient D in cm²/sec, as a function of reciprocal temperature in °K, for several runs of a typical tungsten field emitter. The least squares line $D=D_0e^{-Q/kT}$ is used to determine the values of D_0 and Q.

dynes per cm. Thus the value:

$$\gamma=2900 \text{ dynes/cm} \qquad (10)$$

is proposed for pure tungsten in the solid phase at 2000°K; the uncertainty on this determination of γ is estimated at $\pm10\%$, and results mainly from possible errors in r_0 and F_{01} due to microscope calibration and to approximations in the calculation of F_{01}. Due to the crystalline structure of tungsten, the value of γ is expected to vary with crystallographic orientation and to be lowest for the (110) plane in the present case of a body-centered cubic crystal; however both theoretical and experimental considerations indicate that the variations with crystallographic direction of the surface tension probably do not exceed 10% of the average value. It is of interest to compare our value of γ with the value 2300 dynes/cm recently obtained[17] by the conventional liquid drop technique for tungsten at 3380°K. The values obtained by the two methods appear to be in reasonably good agreement, in view of the expected decrease of the surface tension with increasing temperature.

The experimental dependence of the emitter receding rate on temperature is shown by Fig. 6, which corresponds to several successive runs of a typical emitter. The coordinates have been selected to permit the determination of the surface migration constants D_0 and Q. For this purpose each data point (corresponding to a measurement of dz/dt at a given temperature T) is converted to the corresponding value of $D=D_0e^{-Q/RT}$ by means of Eq. (7); the appropriate values of r and T are used for each experimental point, a value $\gamma=2900$ dynes/cm is used, $\Omega_0=1.57\times10^{-23}$ cm³/atom is obtained from the lattice parameter, and an average value $A_0=10^{-15}$ cm²/atom is used for the surface area per tungsten atom. A plot of $\ln D$ vs $1/T$ shows the straight line expected from the theory; the slope of the experimental line yields the activation energy Q, and the

[17] A. Calverley, Proc. Phys. Soc. (London) **B70**, 1040 (1957).

intercept of the line with the y axis ($1/T=0$) yields the diffusivity constant D_0. Such data has been obtained from several emitters, leading to the following values:

$$Q=3.14\pm0.08 \text{ ev/atom, or } 72 \text{ kcal/mole,}$$
$$D_0=4 \text{ cm}^2/\text{sec.} \quad (11)$$

These values correspond to pure tungsten in the solid phase at an average temperature of 2000°K. The error shown for Q is simply the statistical probable error measuring the scatter in determinations of Q for various emitters. The value of D_0 is probably reliable within a factor 2, the main uncertainty in D_0 resulting from the uncertainty in Q.

The values obtained by the present technique for the physical constants D_0, Q, and γ are well defined and reproducible. However they require interpretation since the crystalline structure of tungsten leads one to expect a variation of its physical properties with crystallographic direction. In the course of an experiment the overall recession of the emitter tip may exceed one thousand atom layers, and atoms removed from the apex of the rounded emitter must migrate over large distances and on surfaces corresponding to a variety of crystallographic orientations. The migration rate is a sensitive function of the activation energy and the rate of the overall process must therefore be controlled by that portion of the total surface migration path with the highest activation energy, at least for the condition of steady flow during which the emitter receding rate is measured. In body-centered cubic crystals directions of the [111] family and planes of the (110) family play a special role as they correspond to the densest packing of atoms. It follows that surface migration in the [111] direction corresponds to an exceptionally low activation energy and occurs most readily; however this direction of migration is possible only on crystal planes such as $(\bar{1}10)$ or $(\bar{2}11)$ for which the sum of Miller indices is zero. In general migration must proceed in a general direction other than [111] or over surfaces which do not contain [111] directions, and a higher activation energy would be expected.

Stranski and Suhrmann[18] have proposed a simple method for estimating the potential energy of surface atoms as a function of location: it is assumed that in first approximation the binding energy between two atoms is a function of their distance only, and is independent of the presence of other neighboring atoms. If ϕ_1 represents the binding energy between nearest neighbors (separated by $r_1=a\sqrt{3}/2$, where a is the lattice parameter, for a body-centered cubic crystal), ϕ_2 represents the binding energy between second nearest neighbors ($r_2=a$), etc., Stranski and Suhrmann have found $\phi_2\cong0.5\phi_1$ and $\phi_3<0.05\phi_1$ for tungsten. Similar values have been obtained by Müller[6] assuming a Van der Waals type of interaction obeying a $(1/r^6)$ law. The known heat of sublimation of tungsten (8.7 ev/atom at 2000°K) may then be used to obtain $\phi_1\cong1.6$ ev. The surface migration of an atom occurs in a succession of individual steps, in each of which the atom leaves a stable site where its potential energy has a minimum E_t and must go over a saddle where its potential energy is E_s in order to reach the next stable site. The corresponding activation energy is simply $Q=2(E_s-E_t)$.

This method has been used to compare the activation energies over the various migration paths in the present experiments where tungsten atoms migrate from the apex toward the shank of a rounded field emitter with its axis parallel to the (110) direction, assuming $\phi_2\cong0.5\phi_1$ after Stranski and Suhrmann and $\phi_n=\phi_2(a/r_n)^6$ for $n>2$. It is found that the initial step in the over-all migration, in which an atom is removed from the edge of the uppermost (110) atom layer, corresponds to an activation energy $Q_0\cong2\phi_1$; the atom then migrates readily over the underlying (110) layer (with $Q\cong\phi_1$) until it becomes attached to the edge of this second layer. However, as the atom proceeds further away from the apex it must migrate over a large number of crystallographic plane facets, such as (100) and (211), for which the activation energy Q is of the order of $2.3\phi_1$ and therefore somewhat larger than Q_0. Such regions determine the over-all migration rate and therefore the activation energy measured for the process, since material cannot accumulate anywhere under the condition of steady-state migration prevailing during the measurements.

The measured activation energy $Q=3.14\pm0.08$ ev/atom thus represents an effective activation energy for the surface migration of tungsten on its own lattice, which is applicable in the general case where the direction of migration does not coincide with a [111] direction and where the crystal surface includes several crystallographic orientations; it also holds approximately for surfaces consisting of a single plane with orientation other than (110). The measured activation energy is somewhat smaller than the calculated value $Q\cong2.3\phi_1\cong3.7$ ev/atom. This discrepancy may be explained by the fact that the calculated value corresponds to the case of an isolated atom migrating over the surface of an ideal crystal, whereas in the experimental case the migration is facilitated by the fact that a large number of atoms participate at a given time, and furthermore experimental evidence indicates that the activation energy for surface migration is reduced by the presence of crystal imperfections such as screw dislocations.

Field emission techniques have been applied to the determination of the physical constants for surface migration. The same techniques may be used in the study of other transport phenomena such as volume self-diffusion, under experimental conditions where volume diffusion predominates. The same general considerations apply, and an expression can be derived for

[18] I. N. Stranski and R. Suhrmann, Ann. Physik **1**, 153 (1947).

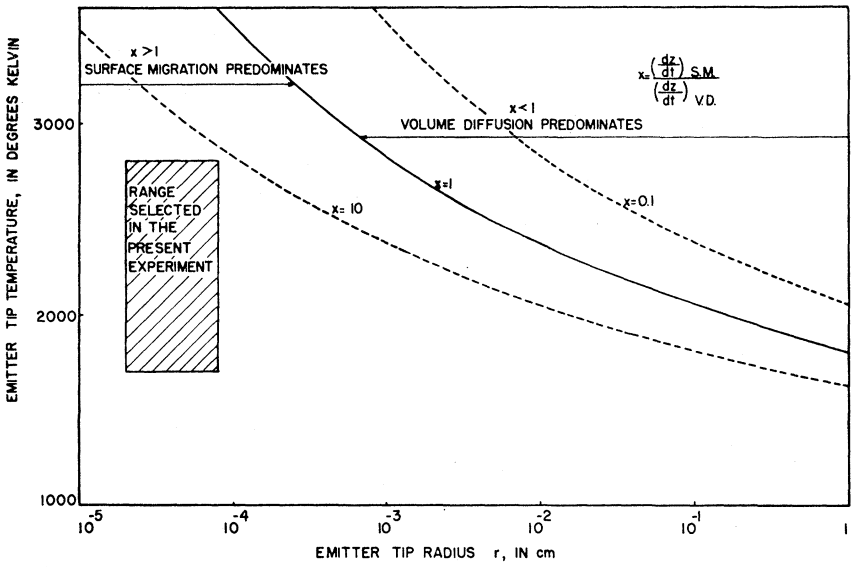

FIG. 7. Comparison of surface migration and volume diffusion rates, for tungsten field cathode.

the emitter receding rate due to volume self-diffusion:

$$\left(\frac{dz}{dt}\right)' = -\gamma\Omega_0 \frac{D_0' e^{-Q'/RT}}{kT} \frac{1.25}{r^2}. \tag{12}$$

The relative magnitude of surface migration and volume diffusion may be estimated from the ratio x of the respective emitter receding rates, given by Eqs. (7) and (12):

$$x = \frac{(dz/dt)_{\text{S.M.}}}{(dz/dt)_{\text{V.D.}}} = \frac{\Omega_0}{A_0} \frac{D_0}{D_0'} e^{(Q'-Q)/RT} \frac{1}{r}, \tag{13}$$

where the primed quantities correspond to volume self-diffusion. It is seen that the relative importance of volume self-diffusion increases as the emitter temperature or radius are increased, since the activation energy Q' for volume diffusion is of course larger than Q. Using the approximate values $D_0' = 11.5$ cm^2/sec and $Q' = 140$ kcal/mole $= 6.1$ ev/atom obtained by Van Liempt[19] for the volume self-diffusion of tungsten, the curves of Fig. 7 are obtained for the ratio x of surface migration to volume diffusion rates. The shade area represents the range of values of r and T used in the present experiment; it falls as expected in the region where surface migration predominates. The study of volume diffusion by the present method would be difficult in the case of tungsten, as it would require both very large cathodes (with correspondingly high emission voltages) and very high surface temperatures, for which evaporation rates would become significant; however the study of volume diffusion by field emission techniques would be possible for materials having a lower ratio of volume diffusion to surface migration activation energy. As noted previously, the process which predominates under given conditions can be identified in a preliminary experiment by the use of Herring's scaling laws.

[19] J. A. M. Van Liempt, Rec. trav. chim. 64, 239 (1945).

V. CONCLUSIONS

The pulsed field emission projection microscope is an effective tool for the quantitative study of self-diffusion processes occurring in single crystals of pure metals. The method can be used for all materials from which field emission can be obtained, and it has the advantage of providing a well-known and controllable geometry as well as criteria for the evaluation of the degree of purity and the crystallographic orientation of the surface under study. Surface migration will usually be the dominant process under the experimental conditions most readily achieved. From the measurement of the receding rate of the field cathode, which can be obtained rapidly and accurately by the ring method, the surface tension γ and the surface migration constants Q and D_0 can be determined with satisfactory accuracy.

ACKNOWLEDGMENT

The authors are grateful to L. M. Perry, F. M. Collins, J. L. Boling, and R. W. Strayer for valuable assistance extended during this work.